NUMERIC MODELING OF THE MAIN ROTOR SPEED UP PROCESS

F .N. Pavlidi
Kamov Company, Moscow

One of the helicopter operational limitations is the maximum allowed wind speed at the main rotor speeding up or stopping.
At relatively low rates of the main rotor rotation that are large enough for blade flapping motion, the blade root portion can strike the droop stop allowing it to deflect only to β_{lim} angle that results in a blade bent along the whole length.
An approximated technique of the main rotor blade section *maximum* bent computation when the blade strikes the droop stop and the results of the main rotor speed up process modeling are presented below. A hinged blade is taken that is elastic enough when striking against the droop stop and absolutely rigid otherwise. The problem is solved in a nonlinear nonstationary setting using a discrete vortex method based on a thin lifting surface theory. It is necessary to note that speed up and stopping of the main rotor are performed at the minimum blade collective pitch angle, i.e. at low load values affecting the rotor disk. Besides, in the conditions under examination relative airflow velocities are large enough. So, according to the analysis, ground effect and inductive interaction of the lower and upper coaxial main rotors is negligible and can be excluded. In a general case relative main rotor speed changes with time according to an arbitrary principle. At each azimuth rotor aerodynamic characteristics are computed [1,6], a blade flap motion differential equation is solved [5] and if the blade strikes the droop stop a bent axis (blade bent) differential equation [3] is solved and each blade flap angle and *maximum* bent of any blade section, tip section included, are defined.
Let us examine a blade rotating around the main rotor axis and making a flapping motion around the flap hinge axis. The blade elements are also affected by aerodynamic, centrifugal and gravity forces (fig. 1).

Let us apply the approach used for calculation of an elastic beam [3] to a blade striking a droop stop.

Let us direct ***X*** axis along the undeformed ("rigid") blade axis and ***Y*** axis from the flap hinge up to the normal to **X** axis as shown in fig. 2 where a simplified blade-to-hub attachment arrangement is presented. Let us examine a blade portion weighing ***dQ***, that elastically shifts to distance δ_d parallel to ***Y*** axis.

Assuming that at the blade stroke all kinetic energy δK of the blade element motion around the flap hinge completely transforms to the elastic blade deformation potential energy δU_d, it can be written:

$$\delta K = \delta U_d \qquad (1)$$

The blade element energy reserve is measured by the work done by it and will amount to:

$$\delta K=\delta A=\delta Q(H+\delta_d)=\delta Q\left(\frac{V^2}{2g}+\delta_d\right) \qquad (2)$$

where:
V – blade element velocity at the initial moment of the stroke;
H – conditional height from which the blade freely falls assuming velocity ***V*** by the moment of the stroke;
g – free fall acceleration.

The expression for potential energy δU_d can be obtained from the following considerations. At static deformation potential energy δU_c is numerically equal to a half of the product of the effective force by the corresponding deformation δ_c:

$$\delta U_c = \frac{1}{2}\delta Q \cdot \delta_c \qquad (3)$$

A static shift of the element under examination can be calculated according to the Hooke 's law:

$$\delta_c=\frac{\delta Q}{C}$$

where:
C – a certain proportion ratio depending upon the blade material, form, size, etc.

Hence, formula (3) can be rewritten as follows:

$$\delta U_c = \frac{C}{2}\delta_c^2.$$

This formula is based on two assumptions:

– correctness of Hooke's law;
– gradual (from zero to the final value) increase of δ_c deformation.

It is clear that while the blade strikes the droop stop, dynamic loading δP_d and blade section shift δ_d increase.

Assuming that both our assumptions are correct and that the stresses created by the dynamic effect of the loads (as it is demonstrated experimentally) do not exceed the material ultimate strength, it can be written:

$$\delta_d=\frac{\delta P_\Delta}{C}=\frac{\delta P_\Delta}{\delta Q}\delta_c \quad \text{and}$$

$$\delta U_d=\frac{1}{2}\delta P_d \cdot \delta_d=\frac{1}{2}\frac{\delta P_\Delta^2}{\delta Q}\delta_c \qquad (4)$$

where:
C – above mentioned proportional ratio retaining its value at the stroke;

Substituting expressions (2) and (4) in equation (1), we get:

$$\delta Q\left(\frac{V^2}{2g}+\frac{\delta P_\Delta}{\delta Q}\delta_c\right)=\frac{1}{2}\frac{\delta P_\Delta^2}{\delta Q}\delta_c\ ,\ \text{or}$$

$$\delta P_d^2-2\,\delta Q\cdot\delta P_d-\frac{dQ^2V^2}{g\delta_c}=0,$$

from where

$$\delta P_d=\delta Q\left(1\pm\sqrt{1+\frac{V^2}{g\delta_c}}\right).$$

Retaining a "plus" sign before the radical to define the maximum deformation value in the direction of the stroke, we obtain:

$$\delta P_d=\delta Q\left(1+\sqrt{1+\frac{V^2}{g\delta_c}}\right),\ \text{or}$$

$$\delta P_d=K_d\cdot\delta Q$$

Here $K_d=1+\sqrt{1+\frac{V^2}{g\delta_c}}$ value presents a dynamic coefficient.

Thus, blade element δQ influences the whole system not through the force of gravity as by static loading but through δP_d force.

Using further D'Alambert principle, allowing to apply an inertial force balanced by active and reactive forces to any point of a body, and considering each blade element and hence the whole blade as being balanced, we can reduce the dynamic problem to a static one.

Since the distance from the flap hinge to the point where the blade comes to rest on the droop stop is small, we can consider the blade be affected at the attachment point by a pair of forces (moment) M_R and reactive forces Y_R, X_R.

Dividing the blade into several sections, replacing the blade attachment with the moment and reactive forces M_R, Y_R, X_R, (fig. 2), knowing a distributed gravity force, obtaining a projection of distributed aerodynamic and centrifugal load in each section, we can calculate the maximum bent of each blade section using an approximated differential equation of elastic line:

$$EJ(x)\,y''=M(x),$$

By integration we obtain a blade bent axis (bents) equation:

$$y=\int\left(\int\frac{M(x)}{EJ(x)}dx\right)dx+\theta_0 x+y_0,$$

where:

θ_0, y_0 - blade section turn and bent angle in the origin of coordinates;

EJ(x) - blade rigidity alternating lengthwise in the general case.

Let us examine all blade sections in a common system of coordinates. We extend all distributed loads to the blade tip introducing compensating loads. Then, considering that the turn angle and section bent in the origin of coordinates are zero and having integrated on constant rigidity and distributed load at each section we obtain:

$$Y(x)=\frac{M_R(x-a)^2}{(EJ)_1 2!}+\frac{Y_R(x-b)^3}{(EJ)_1 3!}+\sum_k\frac{q_k(x-c)^4}{(EJ)_k 4!},$$

where:

M_R, Y_R, q - moment, reactive force and distributed load correspondingly;

a, b, c - distances from the origin of coordinates to M_R, Y_R, q correspondingly

(distance c is taken before the beginning of distributed load).

The maximum tip section bent is:

$$Y_R=\frac{M_R(R-x_f)^2}{(EJ)_1 2!}+\frac{Y_R(R-x_f)^3}{(EJ)_1 3!}+\sum_k\frac{q_k(R-x_f-x_k)^4}{(EJ)_k 4!},$$

where:

R - main rotor radius;

X_f - distance from the main rotor axis to the flap hinge;

x_k - distance from the origin of coordinates to the beginning of distributed load.

When calculating K_d dynamic coefficient the velocity of the blade middle section at the initial moment of the blade stoke against the stop can be found from the following formula:

$$V=\dot{\beta}\cdot r_k,$$

where

r_k - distance from the origin of coordinates to the middle of the blade *k-th* section;

$\dot{\beta}=\frac{\partial\beta}{\partial t}$ - the rate of blade rotation around the flap hinge (known from blade flap motion calculation) and static deformation δ_{ck} is defined experimentally in blade tests.

Results of calculations

Fig. 3-7 present the results of numeric modeling of the Ka-26 helicopter main rotor speed up process and their comparison with experimental data.

Accepted designations

$\bar{n}$ – main rotor relative speed (%);

ω – main rotor rotation rate (rad/s);

R = 6.5 м – main rotor radius;

ω R = 200 m/s – at $\bar{n}$ =100%;

β – blade flap angle (deg);
β_{max} – maximum blade flap angle (deg);
β_{min} – minimum blade flap angle (deg);
h_0 = 1.17 m – distance between the rotors;
Δh_{min} – distance between the planes crossing the upper/lower rotor blade tip sections (m);
Δh – distance between the upper/lower rotor blade tip sections at "meeting azimuths";
W – wind speed (m/s);
$\alpha_{в.}$ = - 6° – rotor setting angle;
LR – lower rotor;
UR – upper rotor;
β_{lim}^{UR} =+0.5° –upper rotor blade droop centrifugal stop angle;
β_{lim}^{LR} =–3.5° – lower rotor blade droop centrifugal stop angle;
ψ =0°, 60°, 120°, 180°, 240°, 300°– upper/lower rotor "meeting azimuths"

The main rotor consists of two coaxial rotors each having three blades of trapesoidal tip configuration.

The calculation starts with $\bar{n}$ =5% (ωR =10 m/s) value maintained for 10 rotor rotations, then the relative rotor speed increases linearly versus time reaching $\bar{n}$ =30% value by the end of the 30-th turn.

Fig. 3 illustrates a vortex structure of a speeding up upper rotor viewed from the top, obtained analytically at W=12 m/s [blade contours, lateral vortices and longitudinal (tip and root) vortices are shown]. The time moment shown in the figure corresponds to $\bar{n} \approx$27%.

Figs. 4 and 5 present blade tip angle β versus azimuth ψ at W=6 m/s and various $\bar{n}$ values and also the minimum distance between the upper/lower rotor blade tips Δh_{min} versus $\bar{n}$ at W=6; 9; 12; 15 and 18m/s and neutral control positions. Curves $\beta(\psi)$ are plotted in a coordinate system connected with the lower rotor so the upper rotor graphs should be read from right to left. On these graphs a solid line presents variation of the blade flap angle versus root section and a dotted line presents the tip section flap angle variation after the blade strikes the droop stop. The dotted line is marked conditionally since only the *maximum* bent is calculated and the corresponding tip section blade angle but not the whole trajectory of the tip section. If the blade does not rest on the droop stop the blade tip and root section, blade root and tip flap angles are assumed to be the same.

The minimum difference between the upper/lower rotor blade tip sections is defined as a distance between the planes crossing the tip sections and perpendicular to the main rotor axis.

$$\Delta h_{min} = h_0 - (h_{max}^{LR} - h_{min}^{UR}) \approx h_0 - R\,(\beta_{max}^{LR} - \beta_{min}^{UR})_{rad}$$

At a small speed of $\bar{n}$ =10% gravity forces prevail and the upper rotor blades rest upon the droop stops for practically a complete rotor turn. The lower rotor blades rest on the stops from $\psi \approx 6\pi/5$ to $\psi \approx \pi/6$. The upper rotor tip section limit angle of deflection from the structure axis of rotation after the stroke against the stop is $\beta_{min}^{UR} = -2{,}5^0$. The maximum value of β_{max}^{LR} does not exceed 1^0. While the $\bar{n}$ increases β_{max} values for both upper and lower rotor increase and shift to $\psi = \pi$ value since the effect of aerodynamic and inertial forces upon the blade becomes more pronounced. At $\bar{n} \geq$15% the lower rotor blades do not reach the blade droop stop already. The upper rotor blade suffer strokes against the droop stop up to $\bar{n}$ =22-23%. The Δh_{min} value reaches its minimum at $\bar{n}$ =16 – 18% (fig. 5). At larger $\bar{n}$ values Δh_{min} value sharply increases in the beginning and at $\bar{n}$ >25% the increase becomes more gradual. Having made calculations for other wind speed values we can plot similar graphs $\Delta h_{min}(\bar{n})$ for various W values (fig.5). Having calculated the same functions for tail wind, we can find minimum Δh_{min} values for various tail wind speeds. The results of these calculations are graphically presented in fig. 6. Evidently, when the tail wind speed increases to W=8m/s, Δh_{min} value reduces to zero. The same Δh_{min} value is reached at the head wind of W=18m/s. Thus, we have obtained the minimum distances between the upper/lower blade tip section planes and can plot a final graph of the limit wind speed distribution versus direction for Δh_{min}=0 (outer curve in fig.7) or, for example, for 20% Δh_{min} reserve margin (inner curve in fig. 7). In this figure arrows show wind speed vector directions and concentric circles show its magnitude. It can be seen that at 20% Δh_{min} reserve margin the head wind should not exceed 13 m/s and the tail wind speed should not exceed 6 m/s. At the same reserve margin the side wind speed (in the direction of 90^0 or 270^0 azimuth) should not exceed 8 m/s, and, for example, a wind in the direction of $150^0 \rightarrow 330^0$ azimuth should not exceed 10 m/s; in the opposite direction at $330^0 \rightarrow 150^0$ in the same conditions the wind speed is limited to 6.5 m/s. For comparison: in [2] wind speed limitations for the Ka-26 helicopter main rotor speed up and stopping are presented as W=16 m/s for head wind, W=8 m/s for side wind and W=3 m/s for tail wind.

Fig. 4 presents also $\beta(\psi)$ at $\bar{n}$ =100% for the lower rotor and $\beta(\psi)$ for the upper rotor at a constant $\bar{n}$ =const=25% that does not change with time. It can be seen that this function differs little from the similar function at $\bar{n}$ =25% but obtained for the rotor speed up.

Fig. 8 presents the experimental results of the Ka-26 main rotor speed up and their correlation with analytical results. During this test a Ka-26 was positioned in another helicopter rotor wake. The flow velocity reached 10-12 m/s, the pedal positions were neutral, the control stick was positioned at X_B=+2/3 of its full travel.

The distances between the upper/lower rotor blade tip sections at the "meeting azimuth" at various $\bar{n}$ values are shown. The scatter of experimental data can evidently be explained by instability of airflow, its vorticity and reflection from the ground. The figures show that everywhere except at azimuth $\psi = 300^0$ experimental and analytical data correlate well. It can also be seen that Δh analytical values slightly exceed experimental ones.

Conclusions

1. An approximated calculation method for maximum bent of the blade section when striking the blade droop stop is developed.

2. The results of numeric modeling of a Ka-26 helicopter main rotor speed up process are presented. Influence of the wind speed and direction on the blade flapping motion during the main rotor speed up with the frequency increasing from $\bar{n}$=5% to $\bar{n}$=30% is investigated. The minimum distances between the upper/lower rotor blade tip sections planes are calculated, the wind speed limit value distribution versus its direction is obtained.

3. The obtained analytical and experimental values show good correlation.

4. The method can be applied for calculations of distances between coaxial helicopter upper/lower rotor tip sections and distances between blade tip sections and airframe components of other design helicopters.

References

1. Белоцерковский С.М., Васин В.А., Локтев Б.Е**. "К построению нестационарной нелинейной теории воздушного винта"**. М., Известия АН СССР, МЖГ, №6, 1979.
2. Лалетин К.Н. **"Практическая аэродинамика вертолета Ка-26"**. М., "Транспорт",1974.
3. Беляев Н.М. **"Сопротивление материалов"**, М., "Наука", 1976.
4. Суриков Н.Ф., Иоффе С.И., Дмитриев А.А., Пак Е.Г. **"Вертолет Ка-26"**. М., "Транспорт", 1982.
5. Аникин В.А., Павлиди Ф.Н. **"О расчете махового движения лопастей винта на неустановившихся режимах полета"**. Научно-методические материалы по прикладным задачам аэродинамики. Вып. I, под ред. Г.Н. Андрейко и А.П. Губчика, изд. ХВВАИУ,1986.
6. Павлиди Ф.Н. **"Расчет нелинейных нестационарных аэродинамических характеристик комбинации "винт - крыло""**. Труды чтений памяти академика Б. Н. Юрьева 13-14 ноября 1989г. Теоретические основы вертолетостроения, МАИ, 1990.

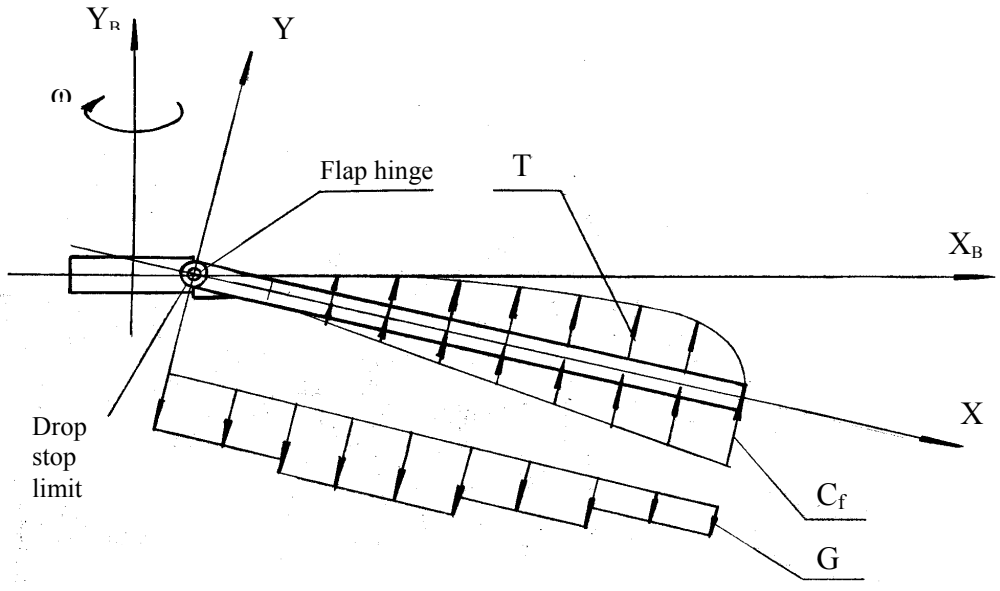

Projections to the normal to the blade axis:
G - of a distributed gravity force load (N/m)
C_f - of a distributed centrifugal force load (N/m)
T - of a distributed aerodynamic load (N/m)

Fig. 1. Forces affecting the blade

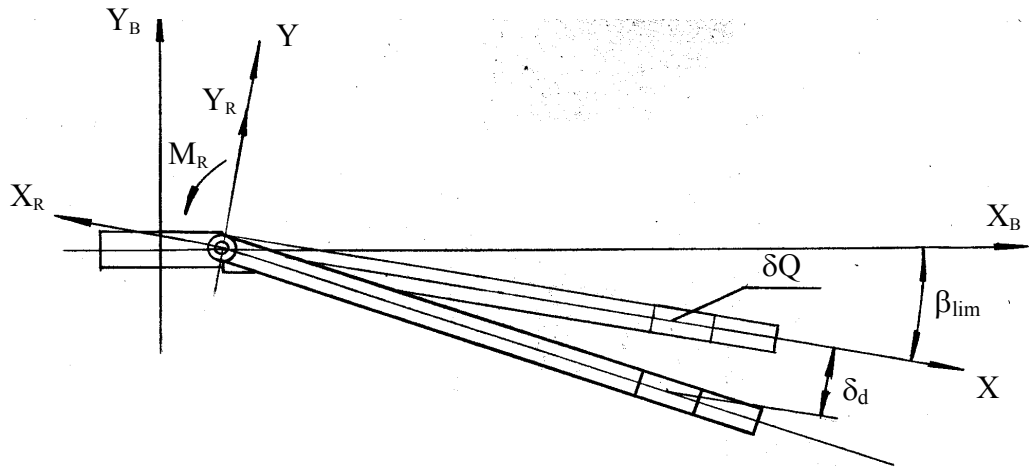

β_{lim} – angle of blade deflection at touching the stop

Fig. 2

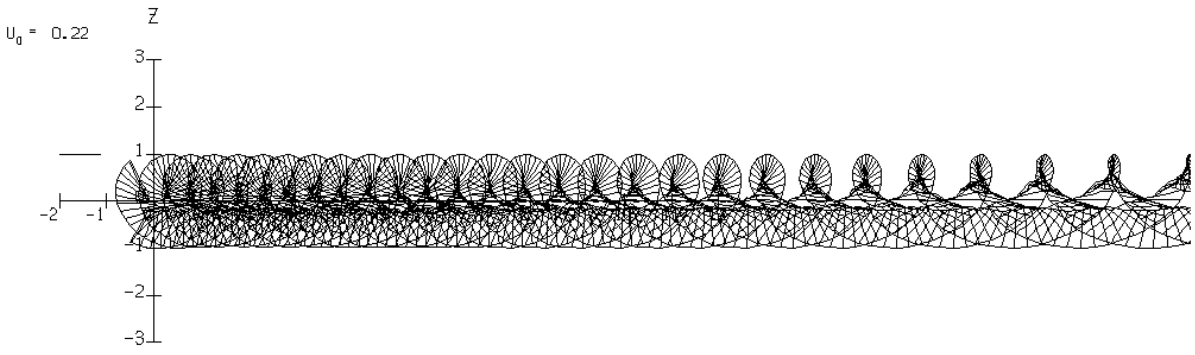

Fig.3

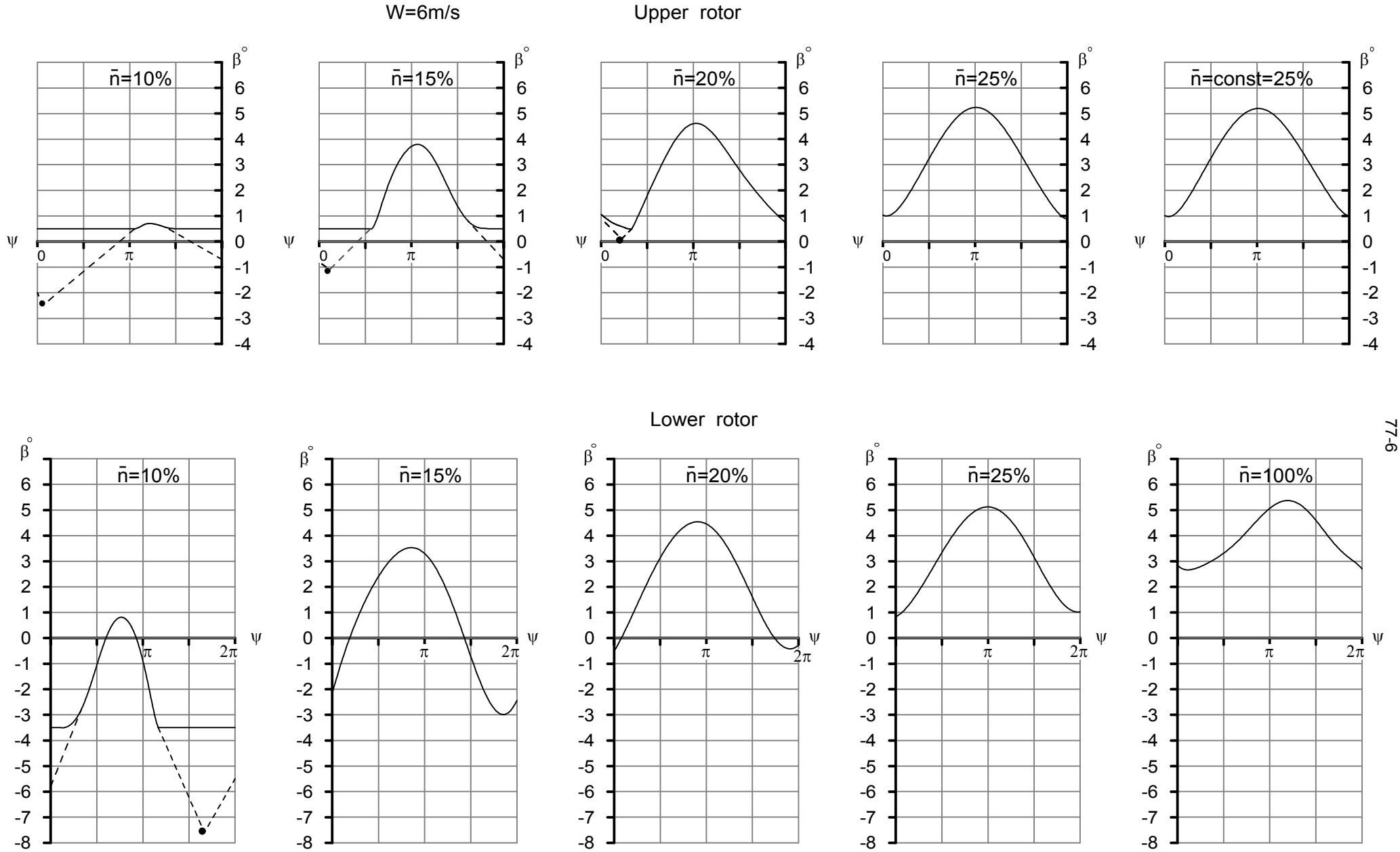
W=6m/s
Upper rotor
n̄=10%
n̄=15%
n̄=20%
n̄=25%
n̄=const=25%
Lower rotor
n̄=10%
n̄=15%
n̄=20%
n̄=25%
n̄=100%
β°
ψ
0
π
2π

Fig.4

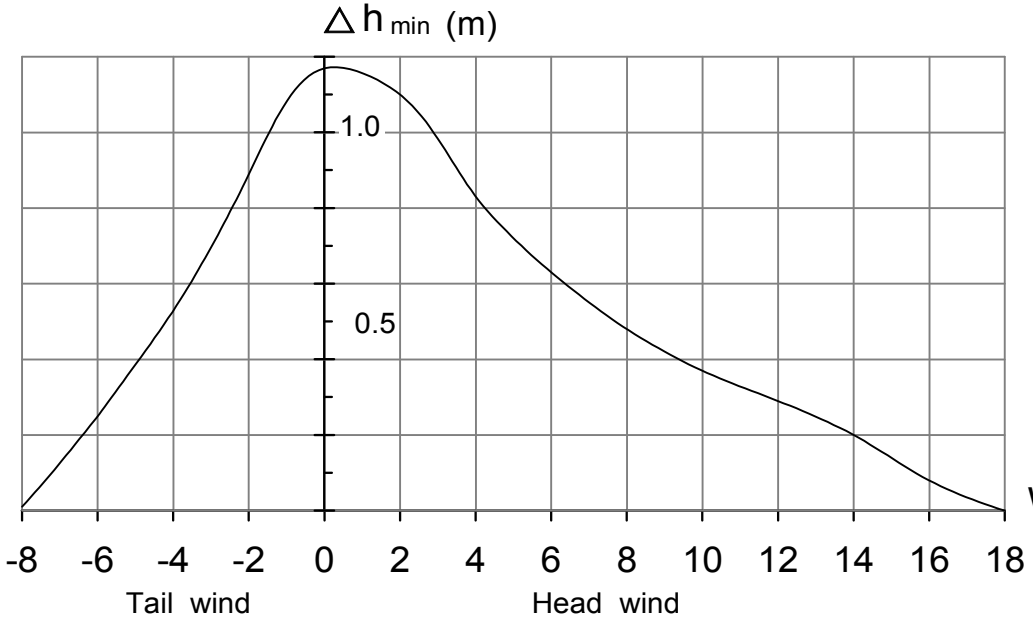

Fig.6

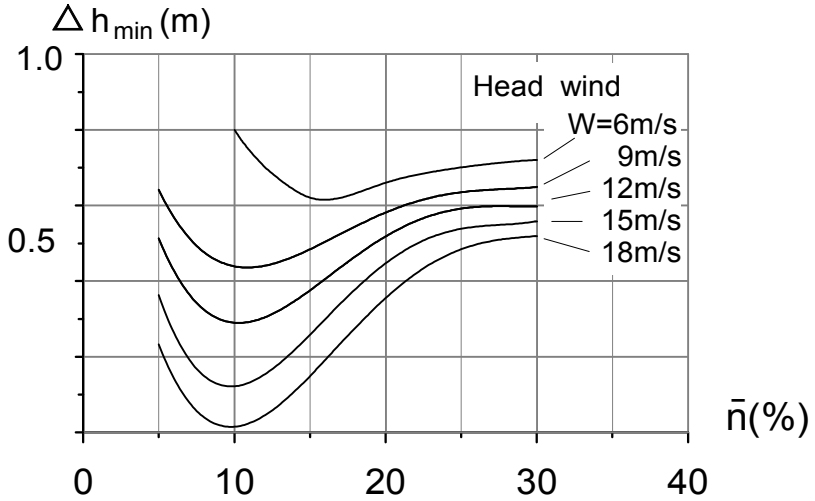

Fig.5

Fig.7

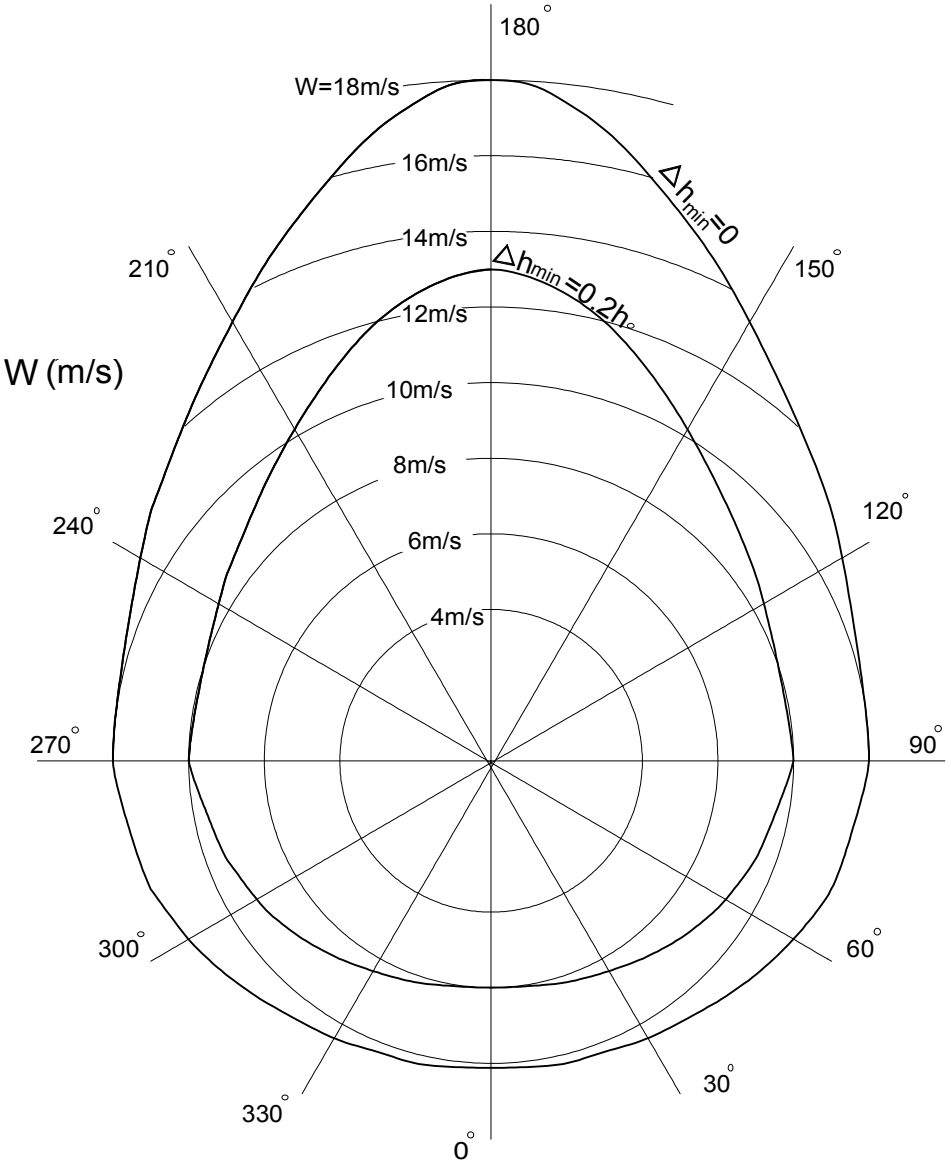

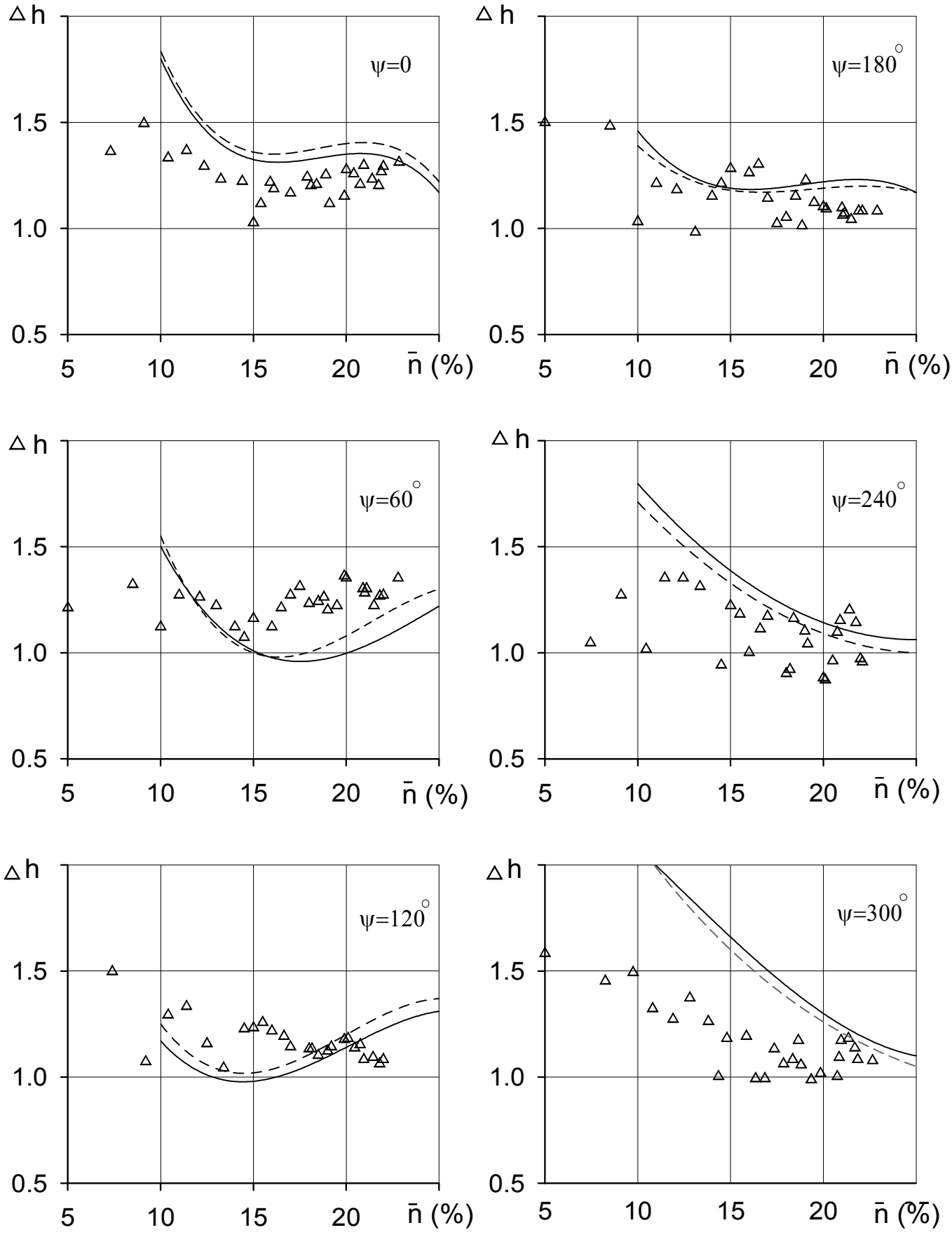
Δh
ψ=0
ψ=180°
ψ=60°
ψ=240°
ψ=120°
ψ=300°
1.5
1.0
0.5
5
10
15
20
n̄ (%)
Δ - experiment, W=10-12 m/s
—— - calculation, W=12 m/s
- - - - - calculation, W=10 m/s

Fig. 8